

TRACE: Transformer-based Risk Assessment for Clinical Evaluation

Dionysis Christopoulos¹, Sotiris Spanos¹, Valsamis Ntouskos^{2,1}, and Konstantinos Karantzas¹

¹National Technical University of Athens

²Universitas Mercatorum

{dxristopoulos,spanosotiris}@mail.ntua.gr, valsamis.ntouskos@unimercatorum.it,
karank@central.ntua.gr

Abstract

We present TRACE (Transformer-based Risk Assessment for Clinical Evaluation), a novel method for clinical risk assessment based on clinical data, leveraging the self-attention mechanism for enhanced feature interaction and result interpretation. Our approach is able to handle different data modalities, including continuous, categorical and multiple-choice (checkbox) attributes. The proposed architecture features a shared representation of the clinical data obtained by integrating specialized embeddings of each data modality, enabling the detection of high-risk individuals using Transformer encoder layers. To assess the effectiveness of the proposed method, a strong baseline based on non-negative multi-layer perceptrons (MLPs) is introduced. The proposed method outperforms various baselines widely used in the domain of clinical risk assessment, while effectively handling missing values. In terms of explainability, our Transformer-based method offers easily interpretable results via attention weights, further enhancing the clinicians’ decision-making process.

1 Introduction

Healthcare is an industry that can gain significantly by utilizing modern artificial intelligence (AI) and machine learning (ML) methods by assisting clinicians in diagnosis, risk assessment and pathology of

diseases. By incorporating AI-driven risk assessment algorithms ([1, 2, 3]), clinicians can offer risk stratification of the patients for screening recommendations, which can help in early detection of diseases, enabling better informed decision-making from the clinicians, on the one hand, and timely intervention for patients that are considered high-risk, on the other.

Healthcare data, typically collected using questionnaire-based surveys, exhibit a large diversity both in the nature, the quantity and the completeness of the attributes that are recorded (or reported) for each patient. Importantly, clinical data are multi-modal, comprising a combination of numerical (i.e., age, height, weight etc.) and categorical features (i.e., eye color, hair color, etc.) or even “checkboxes”, where multiple values within the same feature are valid simultaneously (i.e., ancestry, doctors visited, etc.). On the other hand, missing values and other issues affecting clinical, and tabular data in general, also pose a significant challenge for maximizing data utilization. This is crucial in the case of healthcare data, as they are generally scarce, and their collection is laborious and with high cost, while AI, and deep-learning in particular, typically assume a large quantity of available data for training representative models. Finally, another characteristic of clinical data is the notable imbalance between case and control groups.

These aspects, necessitate the development of task-specific AI and ML methods for the clinical domain. To address the data scarcity, effective methodologies dealing with clinical data should either enhance the data artificially (e.g., through data augmentation/imputation, generative models, etc.) or introduce ways to effectively utilize missing values, inconsistencies, and other issues of the available data. In this work, we propose a transformer-based [4] clinical risk assessment model operating across the spectrum of clinical data feature modalities that explicitly handles missing values, leading to improved performance with minimal computational overhead. Another key contribution of our work is the explainability provided through the generation of attention maps, which facilitates the interpretability of the produced results both for computer scientists and for clinicians.

In summary, the contributions of this work are summarized below:

- We propose a novel framework to perform clinical risk assessment using different data modalities that explicitly handles instances with missing values.
- We introduce “checkbox embeddings” to handle features with multiple valid categories simultaneously, commonly extracted from questionnaire-based surveys.
- The proposed model offers improved explainability, assisting clinicians in interpreting the model results and taking informed decision.
- We establish a new baseline method by deploying a non-negative neural network, inspired by [5] and designed for risk assessment on healthcare clinical data.
- We perform extensive experiments on two clinical datasets for melanoma and heart disease risk assessment, showing that the proposed model, although significantly smaller, achieves competitive performance with respect to the state-of-the-art.

2 Related Work

Risk assessment models have been developed in the healthcare domain, providing risk scores for health condition diagnoses, based on personal clinical data. Logistic regression is a widely used method for such tasks (i.e., primary melanoma classification)[6, 7]. Another study [8] employs various machine learning classifiers like Decision Trees, Polynomial/Rbf/Linear SVM, Naive Bayes, Random Forest and Logistic Regression, as well as a neural network model, aiming to predict type 2 diabetes risk and identifying associated risk factors. Regarding the predictive accuracy, the neural network model, as expected, showcased the best results, suggesting that deep learning models can potentially develop critical decision-making abilities in medical tasks, to enhance prevention on various healthcare chronic conditions. Similarly, [9] employs a single hidden layer MLP network for cardiovascular disease risk prediction, although stating its weak interpretability.

Recent works such as [5, 10] utilize the properties of “non-negative” neural networks, demonstrating their effectiveness on exploring various combinations of potential causes on health outcomes, based on clinical data, or increase the interpretability of medical image analysis, respectively. The architecture proposed in [5] constraints all learnable weights to non-negative values in order to ensure that the existence of an exposure can only increase the risk of the final outcome. In contrast with the weights, biases are constrained to negative values, acting as a threshold, that only allows large weights to pass the activation function and subsequently affect (positively) the final outcome. If a person ends up having no risk contribution to any of the exposures, meaning that the outputs across every node were zeros, then it is assumed that this person has a risk equal to a predefined baseline risk. In our work, we design an improved non-negative neural network as a strong baseline for the task at hand.

Extending the task in other domains, many works shifted towards leveraging Transformer architectures [4], originally designed for Natural Language Processing tasks, to handle tabular data. This shift is motivated through the self-attention mechanism, which provides the Transformer model with the abil-

ity to capture complex feature interactions and dependencies. TabTransformer[11] developed a framework that is composed of a column embedding layer to transform categorical features into learnable vectors. FT-Transformer[12] improves on the previous work, as it deploys a Feature Tokenizer, converting both categorical and numerical features into learnable embeddings. However, there are limitation on these methods such as the handling of missing values. In such cases, Tab-Transformer uses the average of the learned embeddings of all classes within the corresponding column with the missing entries.

Additionally, baseline methods, in order to address class imbalance, utilize oversampling techniques such as SMOTE [13] and CTGAN [14] to generate synthetic samples on the minority class. However, in our approach, we address class imbalance by employing Focal loss, which reduces the need for synthetic data generation.

3 Methods

3.1 Non-negative neural network

Inspired by [5], we develop an architecture that features a three-layer non-negative MLP (nnMLP), intended for baseline comparisons. This design ensures that, during training, weights are constrained to be non-negative. In this context, exposures could either contribute positively to the risk outcome (when $w > 0$) or have no effect (when $w = 0$). Following the baseline, the biases of the two hidden layers are also constrained to be negative, allowing only sufficiently large weights to pass through the activation function, thereby positively affecting the final outcome. However, the bias term of the output layer is left unconstrained, providing additional flexibility in the model. Given the non-negativity of the network’s weights and the utilization of the sigmoid function as the output layer’s activation function, the unconstrained bias provides a baseline risk calculation. Finally, the weight parameters connecting the second hidden layer and the output layer are made learnable. Consequently, the output logit vector is characterized as a weighted sum of the second hidden layer’s acti-

vation outputs, rather than simply aggregating them.

Let i, j, k denote the indices of the nodes in the input layer, the first hidden layer, and the second hidden layer, respectively, $X_{\{1\dots i\}}$ denote the input data features, $Z_{\{1\dots j\}}^1$, $Z_{\{1\dots k\}}^2$ the activation outputs of the first and second hidden layer, respectively. Letting W, b denote the learnable weight parameters and biases of each layer and superscripts $(+), (-)$ the corresponding non-negativity and non-positivity constraints, respectively, equations (1) - (3) describe the operations behind the proposed baseline architecture:

$$Z_j^1 = ReLU \left(\sum_i \left(W_{i,j}^{1(+)} \cdot X_i \right) + b_j^{1(-)} \right), \quad (1)$$

$$Z_k^2 = ReLU \left(\sum_j \left(W_{j,k}^{2(+)} \cdot Z_j^1 \right) + b_k^{2(-)} \right), \quad (2)$$

$$Y = \sum_k \left(W_{k,1}^{3(+)} \cdot Z_k^2 \right) + b^3. \quad (3)$$

It is worth mentioning that *ReLU* is employed as the non-linear activation function on both hidden layers. Additionally, the output logits Y , can be interpreted as probabilities of the positive class outcome, with values in range $[0, 1]$, through the application of the sigmoid activation function.

3.2 TRACE model

The architecture of the proposed Transformer-based Risk Assessment for Clinical Evaluation (TRACE) method is illustrated in Figure 1. It handles various data types encountered in clinical datasets, namely: numerical (continuous), categorical and “checkbox” data. For continuous data, we employ a Multi-Layer Perceptron (MLP), consisting of two linear layers and a SELU activation function between them, to introduce non-linearity. The dimensions of the MLP output are (B, N_{num}, E) where B is the batch size, N_{num} the number of numerical features available on the dataset and E the selected embedding size. Regarding categorical data, we deploy standard categorical

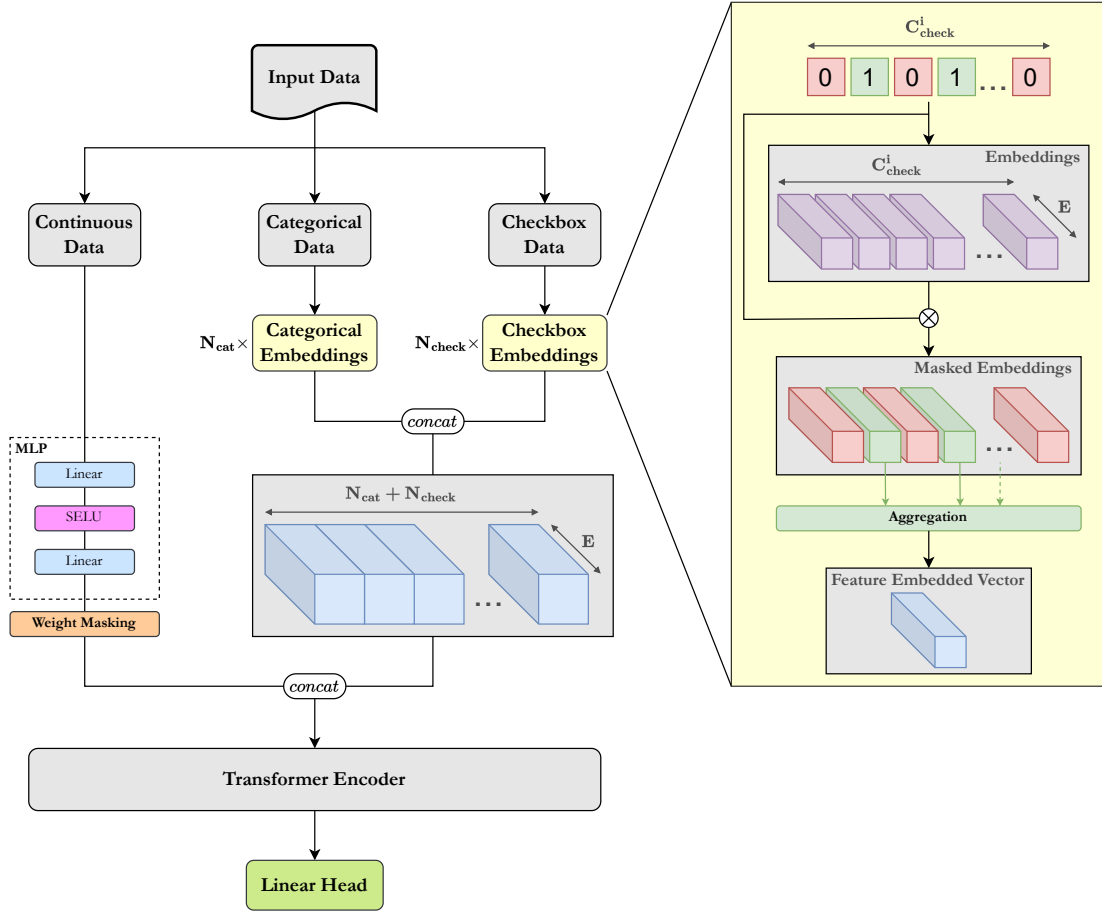


Figure 1: Proposed TRACE architecture. The model supports three types of input data: continuous, categorical, and “checkbox” features. Continuous data is processed through a two-layer MLP with a weight masking mechanism on its outputs. Categorical and “checkbox” data are embedded through their respective embedding layers. All embeddings are concatenated and fed into a transformer encoder block. A linear head can either output logits for binary classification tasks (disease presence or absence), or the risk of developing the disease in a risk assessment task.

embeddings for each feature, ensuring their discrete nature is maintained, while creating the embedded tensor (B, N_{cat}, E) where N_{cat} represents the number of categorical features available in the dataset.

Additionally, we define “checkbox” data, as vectors receiving values 0 or 1, with ones representing the existence of the corresponding category and zeros its

absence, but with the possibility of multiple positive categories on a single feature, thereby making it more complex to handle than standard one-hot encoded data. This type of data are processed with a custom embedding layer, where each checkbox feature is represented as a binary vector of size $C_{checkbox}^i$ corresponding to the total number of possible categories

Table 1: Complete list of the 29 features considered within the melanoma clinical dataset, along with their corresponding descriptions and data types.

Feature Name	Description	Data Type
age at baseline	Age at survey time	continuous
years current residence	Years living in current country at survey time	continuous
height	Height in cm	continuous
weight	Weight in kg	continuous
ancestry (1 to 22)	Ancestry	checkbox
who do you usually see for (1 to 5)	Which doctor do you usually see for skin checks?	checkbox
smoking history	Ever been regular smoker? (smoked daily for at least 6 months)	categorical
smoking history 2	Are you a regular smoker now?	categorical
sex	Sex (as defined at birth)	categorical
current residence	Country of residence at survey time	categorical
marital status	Marital status	categorical
highest qualification	Educational level	categorical
employment	Occupational status at survey time	categorical
occupational exposure	Have your occupations been mainly indoors/outdoors/both?	categorical
clinical skin check	Clinical skin check frequency	categorical
child	How many times were you sunburned badly as a child (under 18 years old)?	categorical
adult	How many times were you sunburned badly as an adult (under 18 years old)?	categorical
sunbed use	How many times have you used sunbeds/tanning beds?	categorical
child sunscreen	Frequency of sunscreen used during summer during childhood (up to 10 years old)	categorical
adolescent sunscreen	Frequency of sunscreen used during summer during adolescence (11-18 years old)	categorical
adult sunscreen	Frequency of sunscreen used during summer during adulthood (over 18 years old)	categorical
hair	Natural hair color at age 21	categorical
eye	Eye color at age 21	categorical
burn	Skin response to sun exposure at noon for 30 minutes without sunscreen/clothing protection	categorical
tan	Does your skin tan after prolonged and repeated sun exposure without sunscreen or clothing?	categorical
freckless	Amount of freckless	categorical
naevi	Naevi in childhood/adolescence (up to 18 years old)	categorical
family history 1st	Have any of your first-degree relatives ever been diagnosed with melanoma?	categorical
family history 2nd	Have any of your second-degree relatives ever been diagnosed with melanoma?	categorical

within the feature for $i \in \{1, \dots, N_{check}\}$. Each category within the i -th checkbox feature, passes through a categorical embedding, resulting in a tensor of size (B, C_{check}^i, E) . Next, an element-wise multiplication is applied between the embedded tensor and the initial binary vector, serving as a mask, zeroing out all the embedded vectors of non-active categories. Subsequently, the active embeddings are aggregated allowing all valid categories to interact with each other, creating a single vector of size E , representing the combined information within the checkbox feature. This process is repeated N_{check} times, resulting in the final embedding tensor (B, N_{check}, E) .

The concatenated embedded tensor $(B, N_{num} + N_{check} + N_{cat}, E)$ integrates all the diverse data representations into a unified feature space, serving as the input to the Transformer Encoder module. This module utilizes the multi-head self-attention mechanism, allowing the model to capture complex rela-

tionships and interactions across the entirety of the features. Finally, a linear head is employed for estimating the risk score.

Finally, the proposed architecture explicitly handles missing values as follows. For continuous data, an element-wise weight masking is applied on the MLP outputs, masking out the weight vectors that correspond to missing numerical values in the input data. For categorical and checkbox data, a special embedding token, is defined for signaling missing values, effectively ignoring these entries.

4 Implementation

4.1 Datasets

Melanoma Clinical Dataset. The first dataset considered in this work is dedicated for first primary melanoma classification and consists of a total

of 415 patient records, with a ratio of 68.7% positive melanoma diagnoses, to 31.3% negative ones. The dataset consists of 29 features (Table 1), four of which contain numerical values, two checkbox-type data, while the rest of them are categorical.

BRFSS Survey Dataset. This study utilizes data from **B**ehavioral **R**isk **F**actor **S**urveillance **S**ystem survey conducted in 2014 and 2022[15]. Following [8], we utilize the 2014 dataset for type 2 diabetes classification, with 139,266 respondents retained, of whom 21,587 have been diagnosed with type 2 diabetes. During preprocessing, 26 features related to this task were selected, while samples containing at least one missing value were ignored. To fully exploit the capabilities of the proposed architecture, we created another version of the same dataset, that retains respondents with missing values and numerical features are maintained as continuous values rather than being converted into categorical variables with arbitrary bins. This version includes 408,599 respondents in total, with 60,538 positive diagnoses. In the same manner, we utilize the 2022 dataset for heart attack/disease classification, with 48 features (Table 2) selected and 440,111 respondents retained in total (39,751 diagnosed with heart attack/disease at least once). A version of this dataset that excludes instances with missing values, indicates a significant drop in the available samples, with just 1,745 respondents remaining.

4.2 Model Training

During training both our proposed networks, we employ Focal loss[16], which can be particularly effective for healthcare clinical datasets, where the case group (disease presence) is significantly outnumbered by the control group (disease absence). Additionally, it emphasizes on hard examples, which in our context, are the false negatives (instances where the model failed to detect a disease), through the Focal loss α hyperparameter. These examples are usually harder to identify, during clinical risk assessment, compared to false positives (instances where the model incorrectly identified a disease) due to class imbalance. The α

value selection, relates to the degree of class imbalance in the dataset.

We train our models in a workstation equipped with an NVIDIA RTX A5000 with 24GB of VRAM. Unless stated otherwise, each TRACE model consists of a single transformer encoder layer, with a global model size of 128. The models were trained for 100 epochs using ADAM optimization algorithm with a learning rate equal to $2e^{-4}$. During training, we ensure that each batch maintains the positive-negative target label ratio of the corresponding dataset. Appendix A provides a more detailed analysis of the training hyperparameters.

5 Experimental Evaluation

In this study we consider five key metrics to evaluate the performance of our trained models: Accuracy, F1-Score, Sensitivity and Specificity and Balanced Accuracy (BA). Accuracy is a straightforward metric, defined as the ratio of correctly predicted examples, both true negatives and true positives, to the total number of instances evaluated. F1-Score is the harmonic mean of Precision and Recall of the positive class to assess the model’s performance on imbalanced datasets. Sensitivity (or Recall) and Specificity are widely used in clinical tasks, illustrating the model’s ability to correctly identify positive and negative instances, respectively, while BA represents their average score.

Tables 3 and 4 compare our proposed method with various baselines on both the melanoma and the BRFSS22 datasets. In particular, two ML methods (Logistic Regression, XGBoost) were considered as baselines, since they are widely used in clinical risk assessment, as well as our proposed non-negative neural network (nnMLP) and FT-Transformer[12] as the current state-of-the-art method for tabular data.

Table 3 represents the results from five runs on the melanoma dataset, each with different random splits, that are consistent across all methods, utilizing a stratified k-fold cross validation. Our model outperforms the baselines in terms of Specificity and Balanced Accuracy (BA) metrics, and achieves the second-best results in Accuracy and F1-Score with

Table 2: Complete list of the 48 features considered within the 2022 BRFSS dataset, after preprocessing, along with their corresponding descriptions and data types.

Feature Name	Description	Data Type
State	State FIPS Code	categorical
Sex	Sex of Respondent	categorical
GeneralHealth	Personal evaluation of General Health	categorical
PhysicalHealthDays	For how many days during the past 30 days was your physical health not good?	continuous
MentalHealthDays	For how many days during the past 30 days was your mental health not good?	continuous
MedicalCost	Was there a time in the past 12 months when you needed to see a doctor but could not because you could not afford it?	categorical
LastCheckupTime	About how long has it been since you last visited a doctor for a routine checkup?	categorical
PhysicalActivities	During the past month did you participate in any physical activities such as running, calisthenics, golf, gardening, or walking for exercise?	categorical
SleepHours	On average, how many hours of sleep do you get in a 24-hour period?	continuous
RemovedTeeth	How many of your permanent teeth have been removed because of tooth decay or gum disease?	categorical
HadStroke	(Ever told) (you had) a stroke.	categorical
HadAsthma	(Ever told) (you had) asthma?	categorical
StillHaveAsthma	Do you still have asthma?	categorical
HadSkinCancer	(Ever told) (you had) skin cancer that is not melanoma?	categorical
HadMelanoma	(Ever told) (you had) melanoma or any other types of cancer?	categorical
HadCOPD	(Ever told) (you had) C.O.P.D. (chronic obstructive pulmonary disease), emphysema or chronic bronchitis?	categorical
HadDepressiveDisorder	(Ever told) (you had) a depressive disorder (including depression, major depression, dysthymia, or minor depression)?	categorical
HadKidneyDisease	Not including kidney stones, bladder infection or incontinence, were you ever told you had kidney disease?	categorical
HadArthritis	(Ever told) (you had) some form of arthritis, rheumatoid arthritis, gout, lupus, or fibromyalgia?	categorical
HadDiabetes	(Ever told) (you had) diabetes?	categorical
Marital	Marital status	categorical
Education	Level of education completed	categorical
Employment	Employment status	categorical
Income	Income categories	categorical
DeafOrHardOfHearing	Are you deaf or do you have serious difficulty hearing?	categorical
BlindOrVisionDifficulty	Are you blind or do you have serious difficulty seeing, even when wearing glasses?	categorical
DifficultyConcentrating	Because of a physical, mental, or emotional condition, do you have serious difficulty concentrating, remembering, or making decisions?	categorical
DifficultyWalking	Do you have serious difficulty walking or climbing stairs?	categorical
DifficultyDressingBathing	Do you have difficulty dressing or bathing?	categorical
DifficultyErrands	Because of a physical, mental, or emotional condition, do you have difficulty doing errands alone such as visiting a doctor's office or shopping?	categorical
SmokerStatus	Four-level smoker status	categorical
ECigaretteUsage	Four-level e-cigarette usage status	categorical
ChestScan	Have you ever had a CT or CAT scan of your chest area?	categorical
RaceEthnicityCategory	Five-level race/ethnicity category	categorical
AgeCategory	Fourteen-level age category	categorical
HeightInMeters	Reported height in meters	continuous
WeightInKilograms	Reported weight in kilograms	continuous
BMI	Body Mass Index (BMI)	continuous
AlcoholDrinkers	Adults who reported having had at least one drink of alcohol in the past 30 days.	categorical
HIVTesting	Adults who have ever been tested for HIV	categorical
FluVaxLast12	During the past 12 months, have you had either flu vaccine that was sprayed in your nose or flu shot injected into your arm?	categorical
PneumoVaxEver	Have you ever had a pneumonia shot also known as a pneumococcal vaccine?	categorical
TetanusLast10Tdap	Have you received a tetanus shot in the past 10 years? Was this Tdap, the tetanus shot that also has pertussis or whooping cough vaccine?	categorical
HighRiskLastYear	HIV high risk for the past 12 months	categorical
HadCovid	Has a doctor, nurse, or other health professional ever told you that you tested positive for COVID 19?	categorical
CovidSymptoms	Did you have any symptoms lasting 3 months or longer that you did not have prior to having coronavirus or COVID-19?	categorical
PrimaryCovidSymptom	Which was the primary COVID-19 symptom that you experienced?	categorical
HeavyDrinkers	Heavy drinkers (adult men having more than 14 drinks per week and adult women having more than 7 drinks per week)	categorical

smaller standard deviations and significantly fewer trainable parameters compared to FT-Transformer. Table 4 represents the results on the BRFSS22 dataset, which introduces a more challenging task due to its highly imbalanced class distribution. In such scenarios, higher accuracy alone may not reflect higher generalization, thus metrics like accuracy and specificity can be misleading, as observed with both ML algorithms. Instead, F1-Score and BA metrics offer a more representative overall assessment of the model's performance. Our proposed model significantly outperforms the baselines regarding the

F1-Score and achieves the second-best BA, just behind the proposed nnMLP. These results demonstrate that our method provides robust and balanced performance across all scenarios.

Table 5 compares the performance of the proposed TRACE model, with the Neural Network from [8] that outperformed all the baselines for the task of type 2 diabetes risk prediction on BRFSS 2014 dataset. Our model was evaluated using different values of the Focal Loss hyperparameter α and as shown, it consistently outperforms the neural network by [8] in several key metrics. More specifically,

Table 3: Comparison of clinical risk assessment algorithms on the melanoma dataset. Average performance metrics and their corresponding standard deviations are reported for each algorithm. Best values are shown in bold and second-best values are underlined.

Method	Accuracy	F1-Score	Sensitivity	Specificity	BA	#Params
Logistic Regression	75.9% \pm 1.7%	0.830 \pm 0.011	0.856 \pm 0.036	0.546 \pm 0.098	70.1% \pm 3.6%	N/A
XGBoost	85.1% \pm 2.5%	0.895 \pm 0.022	<u>0.957</u> \pm 0.020	0.636 \pm 0.060	79.7% \pm 2.5%	N/A
nnMLP	82.4% \pm 2.5%	0.879 \pm 0.015	<u>0.923</u> \pm 0.024	0.608 \pm 0.104	76.5% \pm 4.5%	9,665
FT-Transformer	86.5% \pm 4.5%	0.905 \pm 0.031	0.961 \pm 0.029	<u>0.677</u> \pm 0.156	<u>81.9%</u> \pm 6.5%	3,003,977
TRACE (Ours)	<u>86.0%</u> \pm 3.7%	<u>0.900</u> \pm 0.027	0.941 \pm 0.018	0.709 \pm 0.121	82.5% \pm 5.3%	285,953

Table 4: Comparison of clinical risk assessment algorithms on the BRFSS 2022 dataset. Best values are shown in bold and second-best values are underlined.

Method	Accuracy	F1-Score	Sensitivity	Specificity	BA	#Params
Logistic Regression	91.3%	0.223	0.138	0.990	56.4%	N/A
XGBoost	<u>91.2%</u>	0.209	0.128	0.990	55.9%	N/A
nnMLP	83.0%	0.408	0.649	0.848	74.9%	17,409
FT-Transformer	88.2%	<u>0.416</u>	0.464	<u>0.924</u>	69.4%	2,690,361
TRACE (Ours)	86.6%	0.431	<u>0.564</u>	0.896	<u>73.0%</u>	328,449

Table 5: Comparison of our algorithm with study [8] on the BRFSS 2014 dataset. The dataset was pre-processed based on the guidelines by [8]. For our method, different α values were explored for the Focal loss. Best values are shown in bold and second-best values are underlined.

Method	Accuracy	Sensitivity	Specificity	BA
Neural network[8]	<u>82.4%</u>	0.378	<u>0.902</u>	64.0%
TRACE (Ours), $\alpha = 0.5$	84.1%	0.332	0.934	63.3%
TRACE (Ours), $\alpha = 0.6$	81.8%	0.500	0.877	68.9%
TRACE (Ours), $\alpha = 0.7$	79.4%	<u>0.595</u>	0.831	<u>71.3%</u>
TRACE (Ours), $\alpha = 0.8$	77.2%	0.670	0.790	73.0%

Table 6: Ablation on the proposed checkbox embedding feature for the melanoma dataset.

Model	Accuracy	F1-Score	Sensitivity	Specificity
TRACE w/out checkbox embeddings	84.3% \pm 3.1%	0.888 \pm 0.025	0.954 \pm 0.025	0.632 \pm 0.070
TRACE with checkbox embeddings	86.0% \pm 3.7%	0.900 \pm 0.027	0.941 \pm 0.018	0.709 \pm 0.121

Table 7: Comparison of performance metrics on the BRFSS 2022 dataset, with and without considering missing values during training, across different hyperparameter α values. Both cases utilize the same validation/test set.

Dataset	α	Accuracy	F1-Score	Sensitivity	Specificity	BA	Total Samples
BRFSS 2022 w/out missing values	0.5	83.4%	0.453	0.462	0.899	68.1%	1,745
	0.6	85.7%	0.510	0.500	0.919	71.0%	
	0.7	83.7%	0.496	0.538	0.889	71.4%	
	0.8	80.2%	0.481	0.615	0.835	72.5%	
	0.9	73.6%	0.459	0.750	0.734	74.2%	
BRFSS 2022 with missing values	0.5	87.4%	0.488	0.404	0.956	68.0%	440,111
	0.6	<u>86.5%</u>	<u>0.544</u>	0.538	<u>0.923</u>	73.1%	
	0.7	84.8%	0.555	0.635	0.886	76.1%	
	0.8	77.9%	0.528	<u>0.827</u>	0.771	79.9%	
	0.9	69.6%	0.465	0.885	0.663	<u>77.4%</u>	

for higher α values, our model achieves the best performance in terms of Sensitivity and Balanced Accuracy metrics, reflecting its robustness in identifying positive cases while maintaining a balanced performance across both classes.

Since the TRACE model employs the self-attention mechanism, it offers great insights and interpretability into the decision-making process and results, as visualized by the attention maps in Figures 2 and 3. More specifically, Figure 2 represents the attention weight visualizations for the melanoma (left) and heart disease/attack (right) classification tasks. Its aim is to identify the features that predominantly influence the final positive diagnosis. Rows represent participants randomly selected from the validation set and columns the key features considered during training. Each cell is calculated by averaging the attention weights of each key feature across all input queries. For instance, the frequency of skin checks a patient has, consistently provides high attention weights across the majority of the participants within the melanoma dataset. Similarly, for the heart attack/disease classification task, the participant’s history of CT/CAT scan, C.O.P.D (chronic obstructive pulmonary disease), emphysema, chronic bronchitis, stroke and age category are examples of predominant features. In Figure 3 each cell represents how much

focus to place on each key feature when processing a single query feature, revealing underlying relationships between pairs of features. Diagonal elements typically represent self-attention and high diagonal values indicate that the model is giving significant importance to individual features.

5.1 Ablation

Table 6 explores the impact of our proposed checkbox embedding mechanism, on the melanoma dataset, which includes “checkbox” features. The first row, represents the scenario where checkbox embeddings are not utilized. In this case, each category within the multiple choice features is considered as an independent binary feature and categorical embeddings are applied normally, without any interactions among the categories included in a single feature. The second row, indicates that incorporating checkbox embeddings, improves the model’s performance by capturing interactions within each checkbox feature.

Table 7 compares the performance of our model on the BRFSS 2022 dataset, under two different training scenarios. At first, only samples with complete data are utilized during training (first five rows), resulting in a much smaller dataset with 1,745 samples. On the contrary, the second scenario (last five rows), includes all available samples, by effectively handling missing

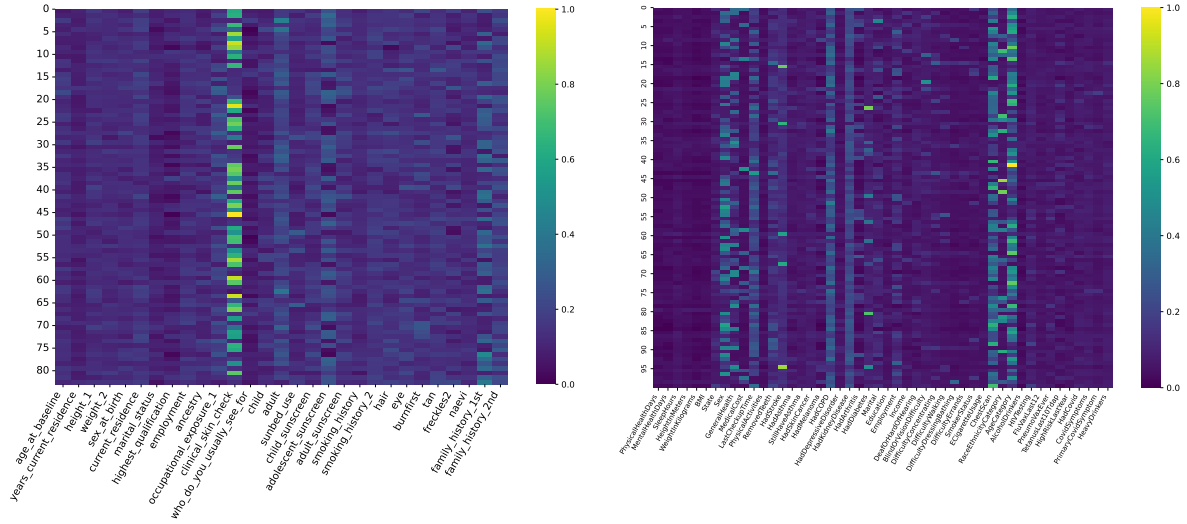


Figure 2: Attention map visualization generated by the TRACE model’s final layer, for the melanoma (left) and BRFSS 2022 (right) dataset, demonstrating the attention weights for each feature. For the BRFSS 2022 dataset, 100 random samples were selected from the validation set. (Best viewed zoomed-in)

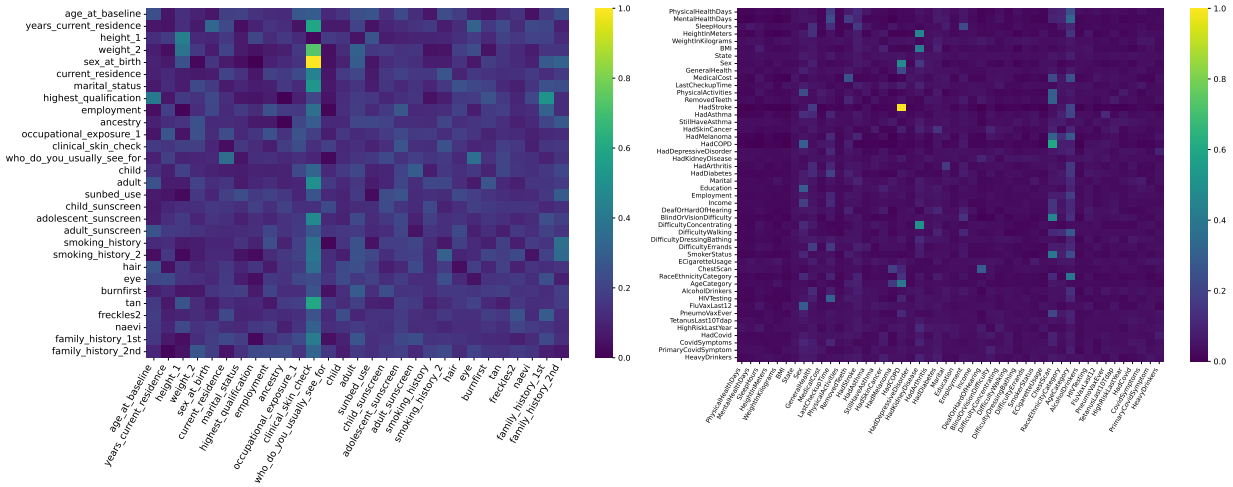


Figure 3: Attention map visualization generated by the TRACE model’s final layer, for the melanoma (left) and BRFSS 2022 (right) dataset, depicting the relationship between queries (rows) and keys (columns). (Best viewed zoomed-in)

features, which increases the total number of samples to 440,111. Both scenarios were evaluated with the same validation set. The results suggest that incorporating additional entries, even affected by missing data, enhances the model’s ability to generalize, improving performance across all metrics.

Figure 4 illustrates the performance of our proposed method (shown on the y axis), across various ratios of randomly simulated missing values (shown on the x axis). Balanced Accuracy captures the combined performance of both Specificity and Sensitivity metrics, while F1-Score reflects the overall performance of the trained model. As expected, higher percentages of missing values (up to 50%) lead to a decline in performance. F1-Score is not significantly affected when up to 30% of the data is masked out. Balanced Accuracy, however, is more sensitive, exhibiting a descending trend, when the percentage of missing values exceeds 5% of the data.

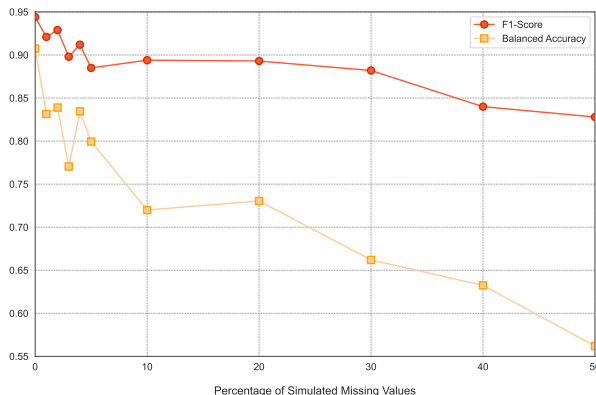


Figure 4: Performance of TRACE in terms of F1-Score and Balanced Accuracy in relation to the ratio of missing values on the melanoma dataset.

6 Conclusions

In this paper, we proposed a novel clinical risk assessment method that utilizes the self-attention mechanism within a Transformer-based architecture. The proposed method, by effectively handling various

data modalities and incomplete data, achieves a competitive performance when compared to state-of-the-art methods while requiring significantly less trainable parameters thus minimizing the computational cost. Additionally, a strong baseline for clinical risk estimation is introduced based on non-negative neural networks (nnMLP), which constrains the network weights to be non-negative, ensuring that the exposure to risk factors only increases the risk of an adverse outcome.

Acknowledgments

This work was supported by the iToBoS EU H2020 project under Grant 965221. We gratefully acknowledge the support of NVIDIA Corporation with the donation of the GPUs used for this research.

References

- [1] J. Yin, K. Y. Ngiam, and H. H. Teo, “Role of artificial intelligence applications in real-life clinical practice: systematic review,” *Journal of medical Internet research*, vol. 23, no. 4, p. e25759, 2021.
- [2] V. K. Shrivastava, N. D. Londhe, R. S. Sonawane, and J. S. Suri, “A novel and robust bayesian approach for segmentation of psoriasis lesions and its risk stratification,” *Computer Methods and Programs in Biomedicine*, vol. 150, pp. 9–22, 2017.
- [3] C. Giordano, M. Brennan, B. Mohamed, P. Rashidi, F. Modave, and P. Tighe, “Accessing artificial intelligence for clinical decision-making,” *Frontiers in digital health*, vol. 3, p. 645232, 2021.
- [4] A. Vaswani, N. Shazeer, N. Parmar, J. Uszkoreit, L. Jones, A. N. Gomez, L. u. Kaiser, and I. Polosukhin, “Attention is all you need,” in *Advances in Neural Information Processing Systems*, I. Guyon, U. V. Luxburg, S. Bengio, H. Wallach, R. Fergus, S. Vishwanathan, and R. Garnett, Eds., vol. 30, 2017.

- [5] A. Rieckmann, P. Dworzynski, L. Arras, S. Lapuschkin, W. Samek, O. A. Arah, N. H. Rod, and C. T. Ekström, “Causes of outcome learning: a causal inference-inspired machine learning approach to disentangling common combinations of potential causes of a health outcome,” *Int. J. Epidemiol.*, vol. 51, no. 5, pp. 1622–1636, Oct. 2022.
- [6] E. Cho, B. A. Rosner, D. Feskanich, and G. A. Colditz, “Risk factors and individual probabilities of melanoma for whites,” *J. Clin. Oncol.*, vol. 23, no. 12, pp. 2669–2675, Apr. 2005.
- [7] K. Vuong, B. K. Armstrong, M. Drummond, J. L. Hopper, J. H. Barrett, J. R. Davies, D. T. Bishop, J. Newton-Bishop, J. F. Aitken, G. G. Giles, H. Schmid, M. A. Jenkins, G. J. Mann, K. McGeechan, and A. E. Cust, “Development and external validation study of a melanoma risk prediction model incorporating clinically assessed naevi and solar lentigines,” *Br. J. Dermatol.*, vol. 182, no. 5, pp. 1262–1268, May 2020.
- [8] Z. Xie, O. Nikolayeva, J. Luo, and D. Li, “Building risk prediction models for type 2 diabetes using machine learning techniques,” *Prev. Chronic Dis.*, vol. 16, no. 190109, p. E130, Sep. 2019.
- [9] S. F. Weng, J. Repts, J. Kai, J. M. Garibaldi, and N. Qureshi, “Can machine-learning improve cardiovascular risk prediction using routine clinical data?” *PLOS ONE*, vol. 12, no. 4, pp. 1–14, 04 2017. [Online]. Available: <https://doi.org/10.1371/journal.pone.0174944>
- [10] V. W. Dauchelle, T. Grenier, F. Durand-Dubief, F. Cotton, and M. Sdika, “Constrained non-negative networks for a more explainable and interpretable classification,” in *Medical Imaging with Deep Learning*, 2024.
- [11] X. Huang, A. Khetan, M. Cvitkovic, and Z. Karnin, “Tabtransformer: Tabular data modeling using contextual embeddings,” 2020.
- [12] Y. V. Gorishniy, I. Rubachev, V. Khrulkov, and A. Babenko, “Revisiting deep learning models for tabular data,” 2021.
- [13] N. V. Chawla, K. W. Bowyer, L. O. Hall, and W. P. Kegelmeyer, “Smote: Synthetic minority over-sampling technique,” *Journal of Artificial Intelligence Research*, vol. 16, p. 321–357, Jun. 2002. [Online]. Available: <http://dx.doi.org/10.1613/jair.953>
- [14] L. Xu, M. Skoularidou, A. Cuesta-Infante, and K. Veeramachaneni, “Modeling tabular data using conditional gan,” in *Advances in Neural Information Processing Systems*, 2019.
- [15] Centers for Disease Control and Prevention (CDC), “Behavioral risk factor surveillance system survey data,” Atlanta, Georgia: U.S. Department of Health and Human Services, Centers for Disease Control and Prevention, 2014, 2022.
- [16] T.-Y. Lin, P. Goyal, R. Girshick, K. He, and P. Dollar, “Focal loss for dense object detection,” in *Proceedings of the IEEE International Conference on Computer Vision (ICCV)*, Oct 2017.

A Focal Loss

Mathematically, Focal loss is defined as:

$$FocalLoss(p_t) = -\alpha_t \cdot (1 - p_t)^\gamma \cdot \log(p_t), \quad (4)$$

where p_t represents the probability corresponding to the true class (disease existence).

It incorporates a modulating factor $(1 - p_t)^\gamma$ on top of the cross entropy loss criterion. This factor forces the model to focus on hard examples, during training. For $\gamma = 0$ Focal loss is equivalent to Cross Entropy, but for $\gamma > 0$ it raises the confidence and subsequently down-weights the contribution of easy examples. In practice, factor α is used as a weighting factor to balance the contribution from both classes, where $0 < \alpha < 1$. Setting α near 0 increases the influence of the negative class, while setting it near 1 the positive class will contribute more to the final result, despite being less represented. The latter scenario aligns with the objective of improving classification of rarely observed instances.

B Training Hyperparameters

For the proposed non-negative MLP network, the default hyperparameters utilized during training are listed in Table 8. We employ a 5-fold stratified k-fold cross validation approach, to ensure that each split maintains the class distribution of the dataset.

Regarding the proposed TRACE model the default hyperparameters used during training, are summarized in Table 9. More specifically we follow a custom sampling pipeline, ensuring that, each batch preserves the target class distribution found in each dataset, in order to mitigate the large contribution of the majority class that leads to overfitting. Each experiment in this study, follows an 80%-20% training-validation split on the melanoma dataset and a 90%-10% ratio on all BRFS dataset versions.

Additionally, categorical data are transformed into one-hot encoded vectors, to meet the input requirements of the non-negative MLP network. In contrast, for the TRACE model, categorical data remain in their original form, with distinct indices assigned on each category and missing values represented with 0 across all features. Finally, during validation and inference steps, we convert the model’s output logits to probabilities using the sigmoid function. This transformation yields the probabilities of the positive class for each instance. We then apply a threshold of 0.5 to perform binary classification, determining whether each instance belongs to the positive or negative class.

We employ “ReduceLROnPlateau” which reduces the learning rate when the balanced accuracy metric (average score of sensitivity and specificity metric) stops improving, with 10 epochs of patience. For both architectures, the best model is determined by the highest F1-Score.

C Extended ablation

Regarding the proposed methodology, exhaustive hyper-parameter optimization has been performed regarding the model size (Table 10) and the encoder layers (Table 11). Increasing the model size and thus the number of trainable parameters did not lead to significant improvements in performance metrics,

Table 8: Default hyperparameters for the proposed non-negative MLP model during training.

Model size	64
Loss function	FL ($\gamma = 2, \alpha = 0.5/0.9$)
Optimizer	RMSProp
Momentum	0.9
Weight decay	$1 \cdot 10^{-3}$
Epochs	100
Learning rate	$2 \cdot 10^{-4}$

Table 9: Default parameters for the proposed TRACE model during training.

Model size	128
No. Transformer encoder layers	1
No. Attention heads	2
Transformer MLP ratio	4
Checkbox embeddings aggregation	“sum”
Final representation	GAP
Loss function	FL ($\gamma = 2, \alpha = 0.5/0.8$)
Optimizer	Adam
Epochs	100
Learning rate	$2 \cdot 10^{-4}$
LR scheduler	ReduceLROnPlateau

leading us to not consider models with sizes greater than 128 from further evaluation. In Table 11, a similar trend was observed when varying the number of transformer encoder layers; increasing the layers did not result in significant performance improvements. Therefore, the study concluded that focusing on models with 64 and 128 sizes, and utilizing fewer encoder layers, is more efficient without sacrificing accuracy.

Figure 5 illustrates the quantitative comparison between our best performing model performance and the FT-Transformer [12] which is the state-of-the-art approach for tabular data. The figure focuses on the trade-off between the F1-score and the number of trainable parameters of the FT-Transformer. In both plots, our method is positioned in the top left, achieving the highest F1-score with the least amount of trainable parameters. Although the F1-scores dif-

Table 10: Ablation on the TRACE model size for the BRFSS 2022 dataset. All models were trained utilizing Focal loss, with α hyperparameter equal to 0.8.

Model Size	Accuracy	F1-Score	Sensitivity	Specificity	BA	Params
64	85.9%	0.432	0.597	0.885	74.1%	90,497
128	86.6%	0.431	0.564	0.896	73.0%	328,449
256	86.1%	0.431	0.584	0.889	73.7%	1,246,721
512	86.1%	0.430	0.583	0.889	73.6%	4,852,737

Table 11: Ablation on the number of transformer encoder layers deployed on the TRACE model for the BRFSS 2022 dataset. The ablation conducted for both 64 and 128 model sizes, while all models were trained utilizing Focal loss, with α hyperparameter equal to 0.8.

Model Size	Enc.layers	Accuracy	F1-Score	Sensitivity	Specificity	BA	Params
64	1	85.9%	0.432	0.597	0.885	74.1%	90,497
	2	86.5%	0.430	0.566	0.894	73.0%	140,481
	3	86.3%	0.430	0.575	0.891	73.3%	190,465
	4	86.5%	0.431	0.567	0.894	73.1%	240,449
128	1	86.6%	0.431	0.564	0.896	73.0%	328,449
	2	86.0%	0.429	0.582	0.888	73.5%	526,721
	3	86.3%	0.429	0.572	0.892	73.2%	724,993
	4	86.9%	0.428	0.545	0.901	72.3%	923,265

fer between the two datasets (melanoma at the top and BRFSS22 at the bottom), the overall trend remains consistent. F1-score in both datasets starts with a decent in F1-score having a high fluctuation around 1.5-2 million parameters and achieves the best score around 3 million. After this point, the performance tends to decline. Our model, consistently outperforms the FT-Transformer in both dataset while maintaining minimal trainable computational overhead. The consistency of these results indicates the effectiveness and robustness of the proposed method.

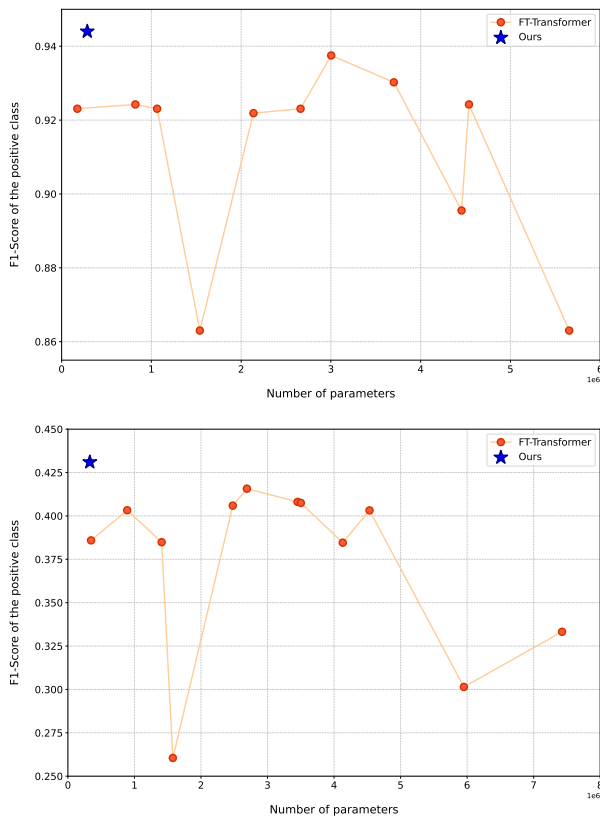


Figure 5: F1-Score vs trainable parameters for both the melanoma (top) and the BRFSS22 (bottom) datasets.